Direct Measurements of Collisional Dynamics in Cold Atom Triads

L. A. Reynolds,[1,2] E. Schwartz,[1,2] U. Ebling,[1,3] M. Weyland,[1,2] J. Brand,[1,3] and M. F. Andersen[1,2,*]

[1] *The Dodd-Walls Centre for Photonic and Quantum Technologies, New Zealand*
[2] *Department of Physics, University of Otago, Dunedin, New Zealand*
[3] *Centre for Theoretical Chemistry and Physics, New Zealand Institute for Advanced Study, Massey University, Auckland, New Zealand*

(Dated: November 24, 2021)

The introduction of optical tweezers for trapping atoms has opened remarkable opportunities for manipulating few–body systems. Here, we present the first bottom–up assembly of atom triads. We directly observe atom loss through inelastic collisions at the single event level, overcoming the substantial challenge in many–atom experiments of distinguishing one-, two-, and three–particle processes. We measure a strong suppression of three–body loss, which is not fully explained by the presently availably theory for three-body processes. The suppression of losses could indicate the presence of local anti–correlations due to the interplay of attractive short range interactions and low dimensional confinement. Our methodology opens a promising pathway in experimental few–body dynamics.

arXiv:2001.05141v1 [quant-ph] 15 Jan 2020

An enduring ambition in atomic physics is to build an understanding of interacting macroscopic systems entirely from knowledge of the underlying microscopic dynamics. In recent years, experimental advancements in isolation and control of single atoms [1–8] paved the way for connecting the few–body and many–body regimes [9]. In particular, optical dipole traps (optical tweezers) proved instrumental in demonstrations of fundamental atomic phenomena like molecular formation and inelastic collisions [10–14]. Conversely, large atomic samples such as Bose–Einstein condensates (BECs) provide a tool for studying atomic dynamics from the many-body perspective [15–18]. Nonetheless, dynamics of large samples are complex with many processes affecting the observed signals simultaneously.

While many phenomena observed in BECs are accurately described in a mean–field framework, the loss processes induced by inelastic particle collisions are strongly influenced by correlations that are omitted in this description [19]. Measured inelastic collision rates therefore provide invaluable information about correlations in a system. Strongly confined repulsive BECs may undergo fermionization with suppressed local correlations leading to reduced atom loss [20–22]. On the contrary, attractive interactions typically lead to a collapse of the condensate [23–25], soliton formation [15, 26–28], or few-body (Efimov) bound states or resonances [16, 29, 30] with enhanced *three-body* loss rates. Three–body recombination happens when three atoms approach within their interaction range, two atoms form a molecule, and the third receives a share of the released binding energy. The process is sensitive to three–particle correlations [20, 21] and has interesting consequences for the many-body dynamics [31], while the accurate modelling of the recombination process is a huge challenge [32]. Three–body recombination occurs throughout physics from ultracold plasmas [33] to chemistry [34] and astrophysics [35] and has been extensively studied in ultracold atoms [22, 36–41]. Moreover, the rich physics of idealised three atom systems in tightly confining traps is currently the target of intensive theoretical studies [42–47], while experiments are presently lacking.

Here we report the first controlled fabrication and manipulation of atom triads via a bottom–up approach of assembling atomic samples. By isolating three independent ^{85}Rb atoms in separate optical tweezers and dynamically bringing them together, we obtain the first experimental observation of distinguishable few–atom inelastic collisions at the single event level. We find a strongly suppressed three–body recombination loss rate compared to previous experiments with many–atom ensembles [40, 41, 48]. There is currently no reliable theory for quantitatively describing three-body processes in an optical tweezer trap. While resonant three-body physics or a modification of the three-body process itself could be relevant, we argue that the suppressed loss rate may indicate the presence of anti-correlations similar to those present in the super-Tonks-Girardeau gas, a metastable phase of attractively interacting bosons in one dimension [49, 50]. We also measure an increased two–body loss which we attribute to photo-assisted processes due to the dipole trap laser field.

Figure 1 portrays the experimental process. It starts by isolating three atoms in three optical tweezers separated by $\sim 4.5\,\mu$m using a similar method as used for two atoms in [11]. The isolation stage utilizes blue–detuned light–assisted collisions yielding a single atom in each tweezer with high probability [51–53]. A high-numerical-aperture lens (NA = 0.55) focuses three steerable linearly polarized laser beams ($\lambda = 1064$ nm) to a spot size of $\omega_0 = 1.1\ \mu$m to form the tweezers. A fluorescence image confirms the presence of the three isolated atoms [11, 54]. The trap oscillation frequencies (measured by Raman sideband spectroscopy) are $\{210, 210, 34\}$ kHz for 110 mW beam power [55]. For other beam powers, the trap frequencies scale with the square root of the power.

Before merging, a σ_- polarized light beam addressing the D_1 $|F=2\rangle$ to $|F'=2\rangle$ transition prepares the atoms in the $|F=2, m_F=-2\rangle$ ground state with 99.1% efficiency. During the preparation, a re–pump beam on the D_2 $|F=3\rangle$ to $|F'=3\rangle$ transition prevents population buildup in the $|F=3\rangle$ state, and a bias magnetic field of 8.5 G defines the quantization axis.

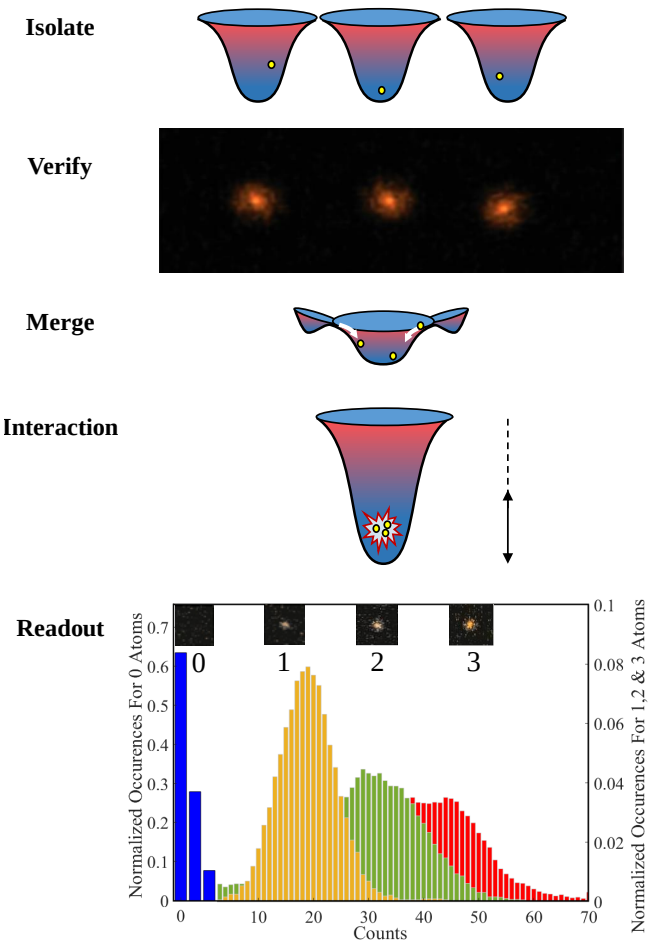


FIG. 1. (Color online) Experimental procedure for directly observing cold atom collisions. We isolate three ^{85}Rb atoms in separate optical tweezers and confirm their presence through fluorescence imaging. A merge and compression stage allows the atoms to interact. Readout: number of photon occurrences for zero (blue), one (yellow), two (green), and three (red) atoms in the tweezer

Using an acousto–optic modulator (AOM), we steer the two outer tweezers closer to the central one until they all merge. The duration of this manipulation is 40 ms, and the final spacing, in merged state, between the centers of the three beams is 0.85 μm. After ramping off the two outermost tweezers adiabatically in ∼30 ms, the single tweezer beam, holding three atoms, ramps adiabatically from 5 mW to 110, 140, 170, or 200 mW. The samples' peak density range is then $0.9-1.5\times10^{14}$ atoms/cm^{-3}. The atoms collide for varying controlled time duration (denoted 'wait time') before the remaining population is determined by using a single photon counting module to detect fluorescence [54, 56]. The 'Readout' section of Fig. 1 shows the photon distributions for 0 (blue), 1 (yellow) 2 (green), or 3 (red) atoms in the single tweezer. The distributions are not entirely separated, but they are sufficiently distinct to allow determination of the probability distribution for each atom number. We fit a weighted sum of them to the measured photon distribution for each wait time. Each photon distribution is sampled from at least 600 experimental repetitions.

The ensemble temperature after merging is 17.8 μK with a tweezer beam power of 5 mW as determined via the release–and–recapture (RR) technique [57]. The temperature scales as the square root of the trap beam power, which allows us to infer the temperature at the 'collision depth'. We verified that the ramp to the collision depth was adiabatic by seeing no significant difference between the temperature before the ramp and after ramping up and back down.

To model atom loss dynamics we use the theory of open quantum systems in the Born–Markov approximation. This is adequate if the atoms are lost from the trap in processes that happen expeditiously relative to the time scale of in–trap dynamics [31]. The Born–Markov master equation for the density operator $\hat{\rho}$ is:

$$\frac{d\hat{\rho}}{dt} = -\frac{i}{\hbar}\left[\hat{H}_T,\hat{\rho}\right] + \sum_{j=1}^{3}\kappa_j\int d^3r\left[2\hat{\psi}^j(\mathbf{r})\hat{\rho}\hat{\psi}^{\dagger j}(\mathbf{r}) - \hat{\psi}^{\dagger j}(\mathbf{r})\hat{\psi}^j(\mathbf{r})\hat{\rho} - \hat{\rho}\hat{\psi}^{\dagger j}(\mathbf{r})\hat{\psi}^j(\mathbf{r})\right], \quad (1)$$

where the coefficients κ_j describe the strength of the j-body loss processes and $\hat{H}_T$ describes the conservative dynamics of the atoms in the trap. When only three or fewer particles are present in the trap, we may derive a set of rate equations for the probabilities $r_i(t)$ for observing i atoms in the tweezer at a given time [58]:

$$\begin{aligned}
\dot{r}_3(t) &= -\Gamma_3 r_3 - 3\widetilde{\Gamma}_2 r_3 - 3\Gamma_1 r_3,\\
\dot{r}_2(t) &= -\Gamma_2 r_2 - 2\Gamma_1 r_2 + 3\Gamma_1 r_3,\\
\dot{r}_1(t) &= -\Gamma_1 r_1 + 3\widetilde{\Gamma}_2 r_3 + 2\Gamma_1 r_2,\\
\dot{r}_0(t) &= \Gamma_3 r_3 + \Gamma_2 r_2 + \Gamma_1 r_1.
\end{aligned} \quad (2)$$

where $\Gamma_1 = 2\kappa_1$. The rate coefficients Γ_j for two- and three–body losses depend on integrated local j-body correlation functions for N particles,

$$\mathcal{C}_N^j \equiv \int d^3r \langle\hat{\psi}^{\dagger j}(\mathbf{r})\hat{\psi}^j(\mathbf{r})\rangle_N \quad (3)$$

and specifically,

$$\Gamma_3 = 2\kappa_3 C_3^3, \quad \Gamma_2 = 2\kappa_2 C_2^2, \quad \widetilde{\Gamma}_2 = \frac{2}{3}\kappa_2 C_2^2. \quad (4)$$

Note that when the three–body coefficient κ_3 is known, a measurement of the rate coefficient Γ_3 constitutes a

measurement of the three–body correlations in the sample. κ_3 can be obtained from measurements or theoretical calculations of the three–body recombination rate coefficient K_3. For the purpose of interpreting our results we use $\kappa_3 = 0.093 \times 10^{-25}\,\mathrm{cm}^6/\mathrm{s}$, which corresponds to the value of K_3 in Ref. [32].

When working with individually assembled triads, the dynamics cease as soon as there is a loss event. This eliminates the need to model a changing density profile as within a large ensemble. We therefore assume the linear rate constants Γ_j to be time independent and extract them from fitting experimental data to the solutions of Eqs. (2) [58].

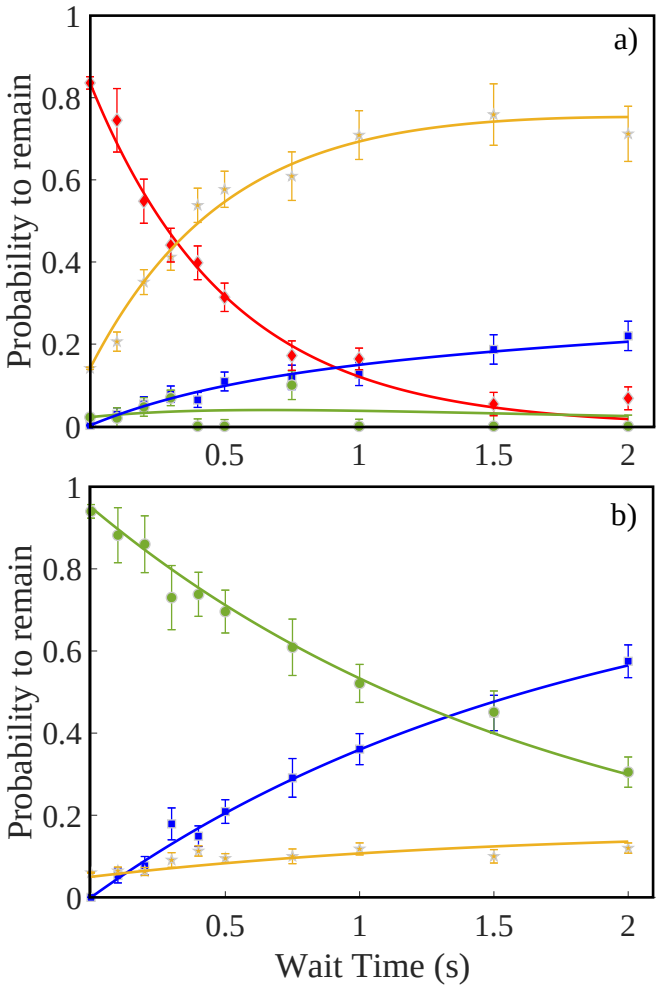


FIG. 2. Measurements of loss dynamics in triads (a) and dyads (b). Measured probability for the remaining atom number being: Three, Red/Diamond; Two, Green/Circle; One, Yellow/Star; Zero Blue/Squares. Solid lines signify a fit to the data with proper Γ_j for triads (Eq. 2) and dyads.

Figure 2 presents example plots of the population dynamics in a tweezer with a beam power of 170 mW. When the probability of observing three atoms in Fig. 2a) (red diamonds) decays, the probabilities for observing one (yellow stars) or zero (blue squares) atoms grows. The probability for observing two atoms remains effectively zero for all times, showing that single-atom loss is negligible in the experiment. The data directly reveal whether a loss event is a three–body event that leads to zero atoms remaining or a two–body event that leads to one atom remaining. The solid lines represent a fit with the solutions to Eq. (2) with $r_j\,(0)$ and Γ_j free parameters.

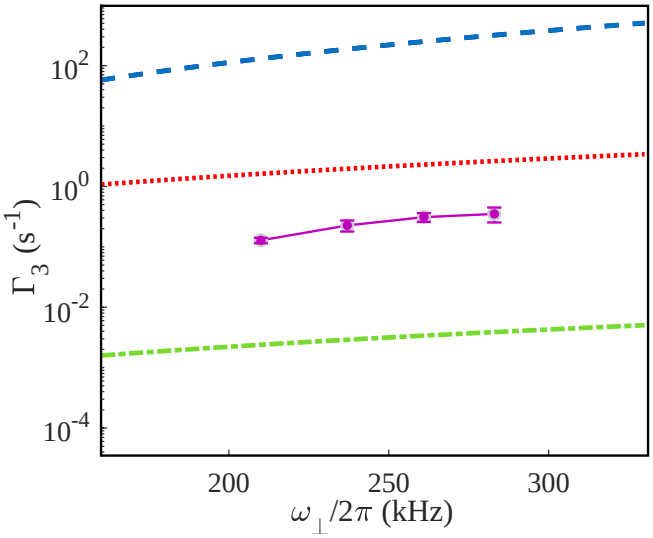


FIG. 3. Comparison of experimentally measured values of the three-body loss rate Γ_3 (purple/solid) with different theoretical models. Blue/dashed: a thermal gas without interaction–induced correlations. Green/dash–dotted: super-Tonks-Girardeau correlations with an integrated thermal density. Red/dotted: Assumes a 1D gas with no occupation of transverse excited modes.

Figure 3 shows how the measured Γ_3 coefficient (purple circles) varies with transverse trap oscillation frequency. We compute C_3^3 for a thermal gas without interaction–induced correlations as ${}^{\mathrm{th}}C_3^3 = \frac{4}{3}\int \mathrm{d}^3r\, n^3(\mathbf{r})$, where the density, $n(\mathbf{r})$, is approximated semi–classically as, $n(\mathbf{r}) = n_0 e^{-V(\mathbf{r})/kT}$, and $V(\mathbf{r})$ is the optical trapping potential. This scenario is considered in previous works [32, 40], with the exception of the pre–factor, which is specific to a three–particle system [58]. The blue dashed line in Fig 3 shows that this prediction lies significantly higher than the measured three–body recombination rate. Equation (4) indicates that a natural candidate for explaining the observed suppression of three–body loss is interaction–induced anti–correlations. Strong anti–correlations are common in one-dimensional (1D) scenarios for both elastic [22] and inelastic [59, 60] interactions, and our tweezer has a high aspect ratio with $\omega_z/\omega_\perp \approx 0.16$. ^{85}Rb's elastic interaction is attractive (negative scattering length, $a = -475a_0$ in this system [61]), where naively the opposite effect is expected. However, anti–correlations occur in the super–Tonks–Girardeau gas, which is an excited state of a one-dimensional (1D) attractive Bose gas

[49, 50], and originate from unrealized two-particle bound states causing an excluded volume similar to the case of hard spheres. In the experiment, a finite temperature of $k_BT \approx 51.37\ \hbar\omega_z$ gives a low statistical weight to the two- and three-particle bound states (solitons), and the situation could be similar to the super–Tonks–Girardeau gas.

To check if super–Tonks–Girardeau–like anti–correlations could be responsible for the three–body loss suppression, we estimate the maximally feasible suppression due to elastic two–body scattering, only. Writing $C_3^3 \approx {g_3}^{\rm th} C_3^3$, the correlation factor $g_3 = \langle\hat{\psi}(z)^{\dagger 3}\hat{\psi}(z)^3\rangle/n(z)^3$, defined for a 1D gas, is $g_3 \approx \frac{16\pi^6}{15\gamma_{\rm LL}^6}$ [20, 62], where $\gamma_{\rm LL} = 2a/[n_{1D}(0)l_\perp^2(1-C\frac{a}{l_\perp})]$ is the dimensionless Lieb-Liniger constant which is a 1D coupling constant with the transverse oscillator length defined as $l_\perp = \sqrt{\hbar/m\omega_\perp}$ ($\mathcal{O}$ 100nm) and $C = 1.0326\ldots$[49]. Taking the maximal transversely integrated particle density for n_{1D} gives the green/dash–dotted line in Fig. 3 and $g_3 \approx 10^{-5}$. This lower bound on Γ_3 shows that super–Tonks–Girardeau–like anti–correlations could be responsible for the suppression.

At our experimental temperature, the sample is not in the transverse ground state of the tweezer, so the green/dash–dotted line likely overestimates the suppression by combining the density–lowering effects of finite temperature and the strongest possible anti–correlations from a 1D theory. The red/dotted line model in Fig. 3 assumes that the atoms are in the transverse ground state before integrating over transverse dimensions in Eq. (3). This gives $C_3^3 \approx \frac{9}{4\pi^4 l_\perp^4}\int \mathrm{d}z\, g_3\, n_{1D}(z)^3$, which yields a three-body loss rate that is slightly higher but closer to the observed rate. While this is predominantly due to the assumed higher atomic density and it does not capture the role played by transversely excited states, the red/dotted line makes a prediction for a possible experiment where the atoms are transversely cooled to the ground state.

In addition to the suppressed three–body rate, Fig. 2a) reveals a high pair loss rate (yellow stars). To confirm that this is indeed a two–body loss process, and not a three–body process where only two of the atoms are lost, we utilize our ability to control the initial atomic population. We switch to initial dyad loading [$r_3(t=0) = 0$, $r_2(t=0) \approx 1$], and obtain population dynamics as in Fig. 2b). Fig. 4 shows $\widetilde{\Gamma}_2$ for triad (red squares) and Γ_2 for dyad (blue circles) loading as a function of transverse trap frequency. Since dyad and triad loading yields $\widetilde{\Gamma}_2 \simeq \Gamma_2$, we conclude that the pair loss observed in Fig. 2a) is the result of a two–body process. By preparing single atoms and observing that they remain in the $|F=2\rangle$ ground state for the experiment duration, we can rule out pair loss from the single-frequency tweezer laser causing spontaneous Raman transitions to the $|F=3\rangle$ ground state, followed by a hyperfine changing collision [12]. Reference [63] showed photo–association resonances in the the vicinity of our tweezer wavelength of 1064 nm. To check if our laser frequency coincidentally is at a photo–association resonance we shifted it by 600 MHz, but nevertheless did not observe a significant change in the pair loss rate. To investigate whether the observed two–body loss may be due to off resonant photo–association [64] as illustrated in the inset of Fig. 4, or a multi–photon process to even higher excited two–atom states [65], we fit the data with models that assume that the two-body rate coefficient $K_2 = \frac{\Gamma_2}{\int \mathrm{d}^3 r\, n^2(\mathbf{r})}$ is proportional to different integer powers of the tweezer beam intensity. The best fit is obtained assuming a quadratic dependence of K_2 on the tweezer beam intensity, which gives $\Gamma_2 = A\omega_\perp^{11/2}$, with A the fitted parameter [58]. This model, shown as the solid line, fits the data well, contrary to models assuming that K_2 is independent or proportional to the tweezer beam intensity. The observed quadratic dependence of K_2 could indicate that the loss involves a two-photon process. For further insight, it would therefore be interesting to change the tweezer beam wavelength in future experiments.

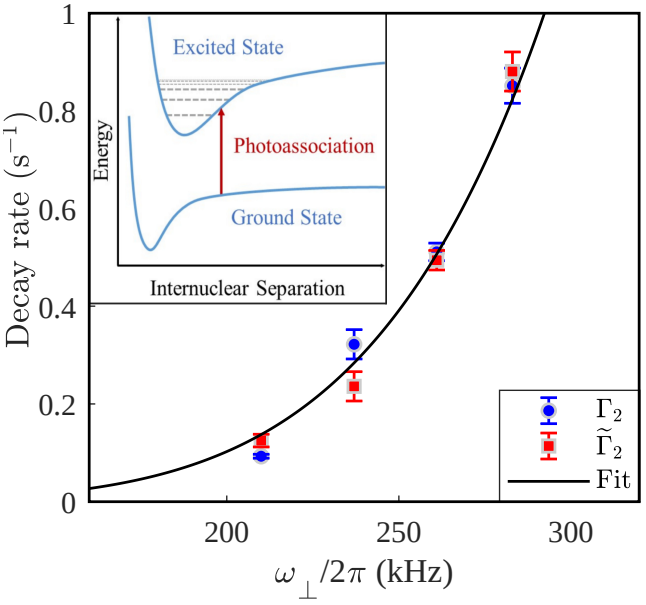


FIG. 4. Measured decay rate using $\widetilde{\Gamma}_2$ for triads (red/square) and Γ_2 for dyads (blue/circle) as a function of trap frequency. *Inset.* illustration of off-resonant photo–association coupling.

By preparing the atoms with random m_F-state in the $|F=2\rangle$ manifold we can measure Γ_3 and Γ_2 with effectively distinguishable bosons. The Γ_3 and Γ_2 coefficients reduced by factors of 0.53 and 0.67 respectively. This is consistent with indistinguishable bosons having a statistical tendency to congregate spatially near each other.

Three–body recombination is problematic in many atomic physics experiments as it results in undesired loss events. It is therefore intriguing that we observe the pro-

cess strongly suppressed. Our present estimations indicate that the suppression could be a result of correlations in the multi-particle wave functions due to a combination of geometric constriction and elastic scattering processes. However, it requires further theoretical developments to verify this, or to clarify whether inelastic three-body processes play a significant role [60]. Here it is interesting to note that we see evidence of inelastic two-body processes, and these may also lead to anti–correlations that suppress loss [59]. An alternative explanation is that the relatively extreme experimental conditions we use alter κ_3. This could happen due to the strong confinement by the tweezer or the presence of the intense tweezer light. Finally, strong transverse confinement affects the Efimov physics of three-body bound states [43] and resonances, and it is presently unknown where these reside for our trap geometry. While the presence of an Efimov resonance would likely rather enhance the three-body loss rate compared to the background, it is also possible that destructive interference between resonant and non–resonant scattering (Fano effect) could reduce the loss rate, as was observed in Ref. [16].

In conclusion, we present the first study of collisional loss dynamics in individually assembled atomic triads. We confirm that all three atoms are lost in three–body recombination, but observe that the rate of the process is strongly suppressed relative to the rate expected from a thermal sample without interaction–induced correlations. Present theory for bulk gases does not fully explain the suppression of three-body loss observed in our experiment but provides a strong indication that interaction-induced anticorrelations cause the effect. Further theoretical developments are needed to understand the dimensional crossover regime that we are probing. Additionally, the data reveal an unexpected two–body loss process induced by the tweezer laser. Our approach overcomes the challenge of differentiating between processes faced when trying to infer few–body dynamics from many-body experiments as well as the need for accurate modelling of a time–dependent density profile. It therefore marks a promising direction for future few–body studies, e.g. the characterisation of Efimov resonances in the dimensional crossover from three to one dimensions by tuning an external magnetic field across a Feshbach resonance.

We gratefully acknowledge comments on our research from a range of members of the scientific community including J. Walraven and D. Blume. This work was supported by the Marsden Fund Council from Government funding, administered by the Royal Society of New Zealand (Contracts No. UOO1835 and MAU1604).

* Email: mikkel.andersen@otago.ac.nz

[1] T Grünzweig, A Hilliard, M McGovern, and MF Andersen, "Near-deterministic preparation of a single atom in an optical microtrap," Nat. Phys. **6**, 951 (2010).
[2] L Isenhower, E Urban, XL Zhang, AT Gill, T Henage, TA Johnson, TG Walker, and M Saffman, "Demonstration of a neutral atom controlled-NOT quantum gate," Phys. Rev. Lett. **104**, 010503 (2010).
[3] S Kuhr, W Alt, D Schrader, M Müller, V Gomer, and D Meschede, "Deterministic delivery of a single atom," Science **293**, 278–280 (2001).
[4] JD Thompson, TG Tiecke, AS Zibrov, V Vuletić, and MD Lukin, "Coherence and Raman sideband cooling of a single atom in an optical tweezer," Phys. Rev. Lett. **110**, 133001 (2013).
[5] J Roßnagel, ST Dawkins, KN Tolazzi, O Abah, E Lutz, F Schmidt-Kaler, and K Singer, "A single-atom heat engine," Science **352**, 325–329 (2016).
[6] D Barredo, S De Léséleuc, V Lienhard, T Lahaye, and A Browaeys, "An atom-by-atom assembler of defect-free arbitrary two-dimensional atomic arrays," Science **354**, 1021–1023 (2016).
[7] M Endres, H Bernien, A Keesling, H Levine, ER Anschuetz, A Krajenbrink, C Senko, V Vuletic, M Greiner, and MD Lukin, "Atom-by-atom assembly of defect-free one-dimensional cold atom arrays," Science **354**, 1024–1027 (2016).
[8] A Goban, RB Hutson, GE Marti, SL Campbell, MA Perlin, PS Julienne, JP DIncao, AM Rey, and J Ye, "Emergence of multi-body interactions in a fermionic lattice clock," Nature **563**, 369–373 (2018).
[9] F Serwane, G Zürn, T Lompe, TB Ottenstein, AN Wenz, and S Jochim, "Deterministic preparation of a tunable few-fermion system," **332**, 336–338 (2011).
[10] P Sompet, AV Carpentier, YH Fung, M McGovern, and MF Andersen, "Dynamics of two atoms undergoing light-assisted collisions in an optical microtrap," Phys. Rev. A **88**, 051401 (2013).
[11] P Sompet, SS Szigeti, E Schwartz, AS Bradley, and MF Andersen, "Thermally robust spin correlations between two ^{85}Rb atoms in an optical microtrap," Nature Communications **10**, 1889 (2019).
[12] P Xu, J Yang, M Liu, X He, Y Zeng, K Wang, J Wang, DJ Papoular, GV Shlyapnikov, and M Zhan, "Interaction-induced decay of a heteronuclear two-atom system," Nat. Commun. **6**, 7803 (2015).
[13] LR Liu, JD Hood, Y Yu, JT Zhang, NR Hutzler, T Rosenband, and K-K Ni, "Building one molecule from a reservoir of two atoms," Science **360**, 900–903 (2018).
[14] BJ Lester, Y Lin, MO Brown, AM Kaufman, RJ Ball, E Knill, AM Rey, and CA Regal, "Measurement-based entanglement of noninteracting bosonic atoms," Phys. Rev. Lett. **120**, 193602 (2018).
[15] SL Cornish, ST Thompson, and CE Wieman, "Formation of bright matter-wave solitons during the collapse of attractive Bose-Einstein condensates," Phys. Rev. Lett. **96**, 170401 (2006).
[16] T Kraemer, M Mark, P Waldburger, JG Danzl, C Chin, B Engeser, AD Lange, K Pilch, A Jaakkola, H-C Nägerl, and R Grimm, "Evidence for Efimov quantum states in an ultracold gas of caesium atoms," Nature **440**, 315–318 (2006).
[17] J Levinsen, MM Parish, and GM Bruun, "Impurity in a Bose-Einstein condensate and the Efimov effect," Phys. Rev. Lett. **115**, 125302 (2015).

[18] CE Klauss, X Xie, C Lopez-Abadia, JP DIncao, Z Hadzibabic, DS Jin, and Eric A Cornell, "Observation of Efimov molecules created from a resonantly interacting Bose gas," Phys. Rev. Lett. **119**, 143401 (2017).

[19] EA Burt, RW Ghrist, CJ Myatt, MJ Holland, EA Cornell, and CE Wieman, "Coherence, Correlations, and Collisions: What one learns about Bose-Einstein condensates from their decay," Phys. Rev. Lett. **79**, 337–340 (1997).

[20] DM Gangardt and GV Shlyapnikov, "Stability and phase coherence of trapped 1D Bose gases," Phys. Rev. Lett. **90**, 010401 (2003).

[21] DM Gangardt and GV Shlyapnikov, "Local correlations in a strongly interacting one-dimensional Bose gas," New J. Phys. **5**, 79 (2003).

[22] BL Tolra, KM OHara, JH Huckans, WD Phillips, SL Rolston, and JV Porto, "Observation of reduced three-body recombination in a correlated 1D degenerate Bose gas," Phys. Rev. Lett. **92**, 190401 (2004).

[23] Y Kagan, AE Muryshev, and GV Shlyapnikov, "Collapse and Bose-Einstein condensation in a trapped Bose gas with negative scattering length," Phys. Rev. Lett. **81**, 933 (1998).

[24] JL Roberts, NR Claussen, SL Cornish, EA Donley, EA Cornell, and CE Wieman, "Controlled collapse of a Bose-Einstein condensate," Phys. Rev. Lett. **86**, 4211 (2001).

[25] CC Bradley, CA Sackett, and RG Hulet, "Bose-Einstein condensation of Lithium: Observation of limited condensate number," Phys. Rev. Lett. **78**, 985 (1997).

[26] KE Strecker, GB Partridge, AG Truscott, and RG Hulet, "Formation and propagation of matter-wave soliton trains," Nature **417**, 150 (2002).

[27] JHV Nguyen, D Luo, and RG Hulet, "Formation of matter-wave soliton trains by modulational instability," Science **356**, 422–426 (2017).

[28] EA Donley, NR Claussen, SL Cornish, JL Roberts, EA Cornell, and CE Wieman, "Dynamics of collapsing and exploding BoseEinstein condensates," Nature **412**, 295 (2001).

[29] V Efimov, "Energy levels arising from resonant two-body forces in a three-body system," Phys. Lett. B **33**, 563–564 (1970).

[30] F Ferlaino, A Zenesini, M Berninger, B Huang, HC Nägerl, and R Grimm, "Efimov Resonances in Ultracold Quantum Gases," Few-Body Syst. **51**, 113–133 (2011).

[31] MW Jack, "Decoherence due to Three-Body Loss and its Effect on the State of a Bose-Einstein Condensate," Phys. Rev. Lett. **89**, 140402 (2002).

[32] BD Esry, CH Greene, and JP Burke, "Recombination of Three Atoms in the Ultracold Limit," Phys. Rev. Lett. **83**, 1751–1754 (1999).

[33] M Lyon and SL Rolston, "Ultracold neutral plasmas," Rep. Prog. Phys. **80**, 017001 (2016).

[34] DL Baulch, CJ Cobos, RA Cox, C Esser, P Frank, Th Just, JA Kerr, MJ Pilling, J Troe, RW Walker, *et al.*, "Evaluated kinetic data for combustion modelling," J. Phys. Chem. Ref. Data **21**, 411–734 (1992).

[35] RC Forrey, "Rate of formation of hydrogen molecules by three-body recombination during primordial star formation," ApJL **773**, L25 (2013).

[36] T Weber, J Herbig, M Mark, H-C Nägerl, and R Grimm, "Three-body recombination at large scattering lengths in an ultracold atomic gas," Phys. Rev. Lett. **91**, 123201 (2003).

[37] N Gross, Z Shotan, S Kokkelmans, and L Khaykovich, "Observation of universality in ultracold Li^7 three-body recombination," Phys. Rev. Lett. **103**, 163202 (2009).

[38] E Braaten and H-W Hammer, "Universality in few-body systems with large scattering length," Phys. Rep. **428**, 259–390 (2006).

[39] JP D'Incao, F Anis, and BD Esry, "Ultracold three-body recombination in two dimensions," Phys. Rev. A **91**, 062710 (2015).

[40] JL Roberts, NR Claussen, SL Cornish, and CE Wieman, "Magnetic field dependence of ultracold inelastic collisions near a Feshbach resonance," Phys. Rev. Lett. **85**, 728 (2000).

[41] PA Altin, GR Dennis, GD McDonald, Daniel Doering, JE Debs, JD Close, CM Savage, and NP Robins, "Collapse and three-body loss in a ^{85}Rb Bose-Einstein condensate," Phys. Rev. A **84**, 033632 (2011).

[42] G Guijarro, A Pricoupenko, GE Astrakharchik, J Boronat, and DS Petrov, "One-dimensional three-boson problem with two- and three-body interactions," Phys. Rev. A **97**, 061605 (2018).

[43] Y Nishida, "Universal bound states of one-dimensional bosons with two- and three-body attractions," Phys. Rev. A **97**, 061603 (2018).

[44] L Pricoupenko, "Pure confinement-induced trimer in one-dimensional atomic waveguides," Phys. Rev. A **97**, 061604 (2018).

[45] L Pricoupenko, "Three-body pseudopotential for atoms confined in one dimension," Phys. Rev. A **99**, 012711 (2019).

[46] M Valiente, "Three-body repulsive forces among identical bosons in one dimension," Phys. Rev. A **100**, 013614 (2019).

[47] L Happ, M Zimmermann, SI Betelu, WP Schleich, and MA Efremov, "Universality in a one-dimensional three-body system," Phys. Rev. A **100**, 012709 (2019).

[48] RJ Wild, P Makotyn, JM Pino, EA Cornell, and DS Jin, "Measurements of Tans contact in an atomic Bose-Einstein condensate," Phys. Rev. Lett. **108**, 145305 (2012).

[49] GE Astrakharchik, J Boronat, J Casulleras, and S Giorgini, "Beyond the Tonks-Girardeau gas: strongly correlated regime in quasi-one-dimensional Bose gases," Phys. Rev. Lett. **95**, 190407 (2005).

[50] E Haller, M Gustavsson, MJ Mark, JG Danzl, R Hart, G Pupillo, and Ngerl H-C., "Realization of an excited, strongly correlated quantum gas phase," Science **325**, 1224–7 (2009).

[51] AV Carpentier, YH Fung, P Sompet, AJ Hilliard, TG Walker, and MF Andersen, "Preparation of a single atom in an optical microtrap," Laser Phys. Lett. **10**, 125501 (2013).

[52] YH Fung and MF Andersen, "Efficient collisional blockade loading of a single atom into a tight microtrap," New Journal of Physics **17**, 073011 (2015).

[53] MO Brown, T Thiele, C Kiehl, T-W Hsu, and CA Regal, "Gray-molasses optical-tweezer loading: Controlling collisions for scaling atom-array assembly," Phys. Rev. X **9**, 011057 (2019).

[54] AJ Hilliard, YH Fung, P Sompet, AV Carpentier, and MF Andersen, "In-trap fluorescence detection of atoms in a microscopic dipole trap," Phys. Rev. A **91**, 053414

(2015).
[55] P Sompet, YH Fung, E Schwartz, MDJ Hunter, J Phrompao, and MF Andersen, "Zeeman-insensitive cooling of a single atom to its two-dimensional motional ground state in tightly focused optical tweezers," Phys. Rev. A **95**, 031403 (2017).
[56] M McGovern, T Grünzweig, AJ Hilliard, and MF Andersen, "Single beam atom sorting machine," Laser Phys. Lett. **9**, 78–84 (2012).
[57] C Tuchendler, AM Lance, A Browaeys, YRP Sortais, and P Grangier, "Energy distribution and cooling of a single atom in an optical tweezer," Phys. Rev. A **78**, 033425 (2008).
[58] See supplemental material at [URL inserted by publisher] for a derivation of the rate Eqs. (2) and their solutions as well as a derivation of the non-interacting few-body correlations functions..
[59] N Syassen, DM Bauer, M Lettner, T Volz, D Dietze, JJ García-Ripoll, JI Cirac, G Rempe, and S Dürr, "Strong dissipation inhibits losses and induces correlations in cold molecular gases," Science **320**, 1329–1331 (2008).
[60] AJ Daley, JM Taylor, S Diehl, M Baranov, and P Zoller, "Atomic Three-Body Loss as a Dynamical Three-Body Interaction," Phys. Rev. Lett. **102**, 040402 (2009).
[61] NR Claussen, SJJMF Kokkelmans, ST Thompson, EA Donley, E Hodby, and CE Wieman, "Very–high–precision bound–state spectroscopy near a ^{85}Rb Feshbach resonance," Phys. Rev. A **67**, 060701 (2003).
[62] M Kormos, G Mussardo, and A Trombettoni, "Local correlations in the super-Tonks-Girardeau gas," Phys. Rev. A **83**, 013617 (2011).
[63] HF Passagem, R Colin-Rodriguez, PCV da Silva, N Bouloufa-Maafa, O Dulieu, and LG Marcassa, "Formation of ultracold molecules induced by a high-power single-frequency fiber laser," J. Phys. B: At., Mol. Opt. Phys. **50**, 045202 (2017).
[64] KM Jones, E Tiesinga, Paul D Lett, and PS Julienne, "Ultracold photoassociation spectroscopy: Long-range molecules and atomic scattering," Rev. Mod. Phys. **78**, 483–535 (2006).
[65] M Schlagmüller, TC Liebisch, F Engel, KS Kleinbach, F Böttcher, U Hermann, KM Westphal, A Gaj, R Löw, S Hofferberth, T Pfau, J Pérez-Ríos, and CH Greene, "Ultracold chemical reactions of a single Rydberg atom in a dense gas," Phys. Rev. X **6**, 031020 (2016).

SUPPLEMENTAL MATERIAL

FROM MASTER EQUATION TO RATE EQUATIONS

In this work we model atom loss dynamics using the theory of open quantum system in the Born-Markov approximation, which is adequate if the atoms are completely lost from the trap in processes that happen quickly compared to the time-scale of in-trap dynamics [31]. The Born-Markov master equation for the many-body density operator $\hat{\rho}$ is then given by

$$\frac{d\hat{\rho}}{dt} = -\frac{i}{\hbar}\left[\hat{H}_T, \hat{\rho}\right] + \sum_{j=1}^{3} \kappa_j \int d^3r \left[2\hat{\psi}^j(\mathbf{r})\hat{\rho}\hat{\psi}^{\dagger j}(\mathbf{r}) - \hat{\psi}^{\dagger j}(\mathbf{r})\hat{\psi}^j(\mathbf{r})\hat{\rho} - \hat{\rho}\hat{\psi}^{\dagger j}(\mathbf{r})\hat{\psi}^j(\mathbf{r})\right], \tag{5}$$

with the non-dissipative part given by the commutator and three Lindblad-type terms for 1,2,3-body losses.

To go from here to equations for probabilities, we first separate the density matrix into its $0, 1, 2, \ldots$-particle components:

$$\hat{\rho} = r_0\hat{\rho}_0 + r_1\hat{\rho}_1 + r_2\hat{\rho}_2 + r_3\hat{\rho}_3 + \ldots. \tag{6}$$

We define the full density matrix as well as each partial n-body component to be normalized, such that

$$\mathrm{Tr}\,\hat{\rho} = 1, \tag{7}$$
$$\mathrm{Tr}\,\hat{\rho}_i = 1, \tag{8}$$

and therefore the coefficients must obey

$$\sum_i r_i = 1, \tag{9}$$

and can be interpreted as probabilities. We now define the projection operator

$$\hat{P}_n = \sum_\nu |\nu, n\rangle\langle\nu, n|, \tag{10}$$

where the sum over ν denotes a sum over all states in the n-body subspace of the Hilbert space. This means, that

$$\hat{P}_n\hat{\rho} = r_n\hat{\rho}_n \tag{11}$$

and $\hat{P}_n^2 = \hat{P}_n$. The n-body subspaces are orthogonal, therefore

$$\hat{P}_n\hat{\rho}_k = \delta_{kn}\hat{\rho}_k \quad \& \quad \left[\hat{P}_n, \hat{\rho}_k\right] = 0. \tag{12}$$

If we apply this projector to the full Master equation (5) above, we can split it into equations for each n-body component. We obtain

$$\begin{aligned}\hat{P}_n\frac{d\hat{\rho}}{dt} &= -\frac{i}{\hbar}r_n\left[H_T, \hat{\rho}_n\right] + \sum_{j=1}^{3}\kappa_j\int d^3r\hat{P}_n\left[2\hat{\psi}^j\hat{\rho}\hat{\psi}^{\dagger j} - \hat{\psi}^{\dagger j}\hat{\psi}^j\hat{\rho} - \hat{\rho}\hat{\psi}^{\dagger j}\hat{\psi}^j\right] \\ &= -\frac{i}{\hbar}r_n\left[H_T, \hat{\rho}_n\right] + \sum_{j=1}^{3}\kappa_j\int d^3r\left[2\hat{\psi}^j\hat{\rho}_{n+j}r_{n+j}\hat{\psi}^{\dagger j} - \hat{\psi}^{\dagger j}\hat{\psi}^j\hat{\rho}_n r_n - \hat{\rho}_n r_n\hat{\psi}^{\dagger j}\hat{\psi}^j\right].\end{aligned} \tag{13}$$

Now, we take the trace of this equation. For the left hand side, we obtain

$$\mathrm{Tr}\,\hat{P}_n\frac{d\hat{\rho}}{dt} = \frac{d}{dt}\mathrm{Tr}\,\hat{P}_n\hat{\rho} = \frac{d}{dt}\mathrm{Tr}\,r_n\hat{\rho}_n = \frac{d}{dt}r_n, \tag{14}$$

because of the normalization of $\hat{\rho}_n$. The non-dissipative term on the right hand side vanishes, since $\mathrm{Tr}[A, B] = 0$. What remains is the following expression

$$\frac{d}{dt}r_n = \sum_{j=1}^{3}\kappa_j\left\{\mathrm{Tr}\left[2\int d^3r\hat{\psi}^j\hat{\rho}_{n+j}\hat{\psi}^{\dagger j}\right]r_{n+j} - \mathrm{Tr}\left[\int d^3r\hat{\psi}^{\dagger j}\hat{\psi}^j\hat{\rho}_n\right]r_n - r_n\mathrm{Tr}\left[\int d^3r\hat{\rho}_n\hat{\psi}^{\dagger j}\hat{\psi}^j\right]\right\}. \tag{15}$$

Using the cyclic property of the trace, we can simplify this expression and obtain coupled rate equations for the probabilities r_n,

$$\frac{d}{dt}r_n = 2\sum_{j=1}^{3}\kappa_j\left\{r_{n+j}\int d^3x\mathrm{Tr}\left[\hat{\psi}^{\dagger j}\hat{\psi}^j\hat{\rho}_{n+j}\right] - r_n\int d^3x\mathrm{Tr}\left[\hat{\psi}^{\dagger j}\hat{\psi}^j\hat{\rho}_n\right]\right\}. \tag{16}$$

The coefficients are given by expectation values of products of field operators in the n-body subspace of the Hilbert space, which we denote by

$$\langle\hat{O}\rangle_n = \mathrm{Tr}\left(\hat{O}\hat{\rho}_n\right). \tag{17}$$

With this notation and re-adding the explicit $\mathbf{r}$-dependence of the fields, the equation above reads as

$$\frac{d}{dt}r_n = 2\sum_{j=1}^{3}\kappa_j\left(r_{n+j}\int d^3r\langle\hat{\psi}^{\dagger j}(\mathbf{r})\hat{\psi}^j(\mathbf{r})\rangle_{n+j} - r_n\int d^3r\langle\hat{\psi}^{\dagger j}(\mathbf{r})\hat{\psi}^j(\mathbf{r})\rangle_n\right). \tag{18}$$

Rate equations for probabilities

Let us now explicitly write down rate equations for the a 3-body system with just the probabilities r_n, $n = 0, 1, 2, 3$. First, we have

$$\begin{aligned}\dot{r}_0 &= 2\kappa_1\left(r_1\int d^3r\langle\hat{\psi}^\dagger(\mathbf{r})\hat{\psi}(\mathbf{r})\rangle_1 - r_0\int d^3r\langle\hat{\psi}^\dagger(\mathbf{r})\hat{\psi}(\mathbf{r})\rangle_0\right) \\ &+ 2\kappa_2\left(r_2\int d^3r\langle\hat{\psi}^{\dagger 2}(\mathbf{r})\hat{\psi}^2(\mathbf{r})\rangle_2 - r_0\int d^3r\langle\hat{\psi}^{\dagger 2}(\mathbf{r})\hat{\psi}^2(\mathbf{r})\rangle_0\right) \\ &+ 2\kappa_3\left(r_3\int d^3r\langle\hat{\psi}^{\dagger 3}(\mathbf{r})\hat{\psi}^3(\mathbf{r})\rangle_3 - r_0\int d^3r\langle\hat{\psi}^{\dagger 3}(\mathbf{r})\hat{\psi}^3(\mathbf{r})\rangle_0\right),\end{aligned} \tag{19}$$

where we quickly note that the loss terms on the right (with the minus sign) all vanish, because $\langle\hat{\psi}^{\dagger n}\hat{\psi}^{n}\rangle_m = 0$ for $m < n$. Also, we use

$$\int d^3r\langle\hat{\psi}^\dagger(\mathbf{r})\hat{\psi}(\mathbf{r})\rangle_m = \mathrm{Tr}\int d^3r\hat{\psi}^\dagger(\mathbf{r})\hat{\psi}(\mathbf{r})\hat{\rho}_m = m\,\mathrm{Tr}\,\rho_m = m. \tag{20}$$

to reduce this equation to

$$\dot{r}_0 = 2\kappa_1 r_1 + 2\kappa_2 r_2\int d^3r\langle\hat{\psi}^{\dagger 2}(\mathbf{r})\hat{\psi}^2(\mathbf{r})\rangle_2 + 2\kappa_3 r_3\int d^3r\langle\hat{\psi}^{\dagger 3}(\mathbf{r})\hat{\psi}^3(\mathbf{r})\rangle_3. \tag{21}$$

Analogously, we compute the remaining rate equations for r_n, $n = 1, 2, 3$:

$$\dot{r}_1 = 2\kappa_1(2r_2 - r_1) + 2\kappa_2 r_3\int d^3r\langle\hat{\psi}^{\dagger 2}(\mathbf{r})\hat{\psi}^2(\mathbf{r})\rangle_3 \tag{22}$$

$$\dot{r}_2 = 2\kappa_1(3r_3 - 2r_2) - r_2\int d^3r\langle\hat{\psi}^{\dagger 2}(\mathbf{r})\hat{\psi}^2(\mathbf{r})\rangle_2 \tag{23}$$

$$\dot{r}_3 = 2\kappa_1(4r_4 - 3r_3) - r_3\int d^3r\langle\hat{\psi}^{\dagger 2}(\mathbf{r})\hat{\psi}^2(\mathbf{r})\rangle_3 - r_3\int d^3r\langle\hat{\psi}^{\dagger 3}(\mathbf{r})\hat{\psi}^3(\mathbf{r})\rangle_3. \tag{24}$$

If we define a shorthand for the integral over the local n-body correlation function in the m-body subspace

$$\mathcal{C}_m^n \equiv \int d^3r\langle\hat{\psi}^{\dagger n}(\mathbf{r})\hat{\psi}^n(\mathbf{r})\rangle_m, \tag{25}$$

we obtain the following set of equations:

$$\begin{aligned}
\dot{r}_0(t) &= \Gamma_3 r_3 + \Gamma_2 r_2 + \Gamma_1 r_1,\\
\dot{r}_1(t) &= -\Gamma_1 r_1 + \widetilde{\Gamma}_2(3r_3) + \Gamma_1(2r_2),\\
\dot{r}_2(t) &= -\Gamma_2 r_2 - \Gamma_1(2r_2) + \Gamma_1(3r_3),\\
\dot{r}_3(t) &= -\Gamma_3 r_3 - \widetilde{\Gamma}_2(3r_3) - \Gamma_1(3r_3),
\end{aligned} \tag{26}$$

where substituting

$$\Gamma_1 = 2\kappa_1, \tag{27}$$

yields Eq. (2) in the paper and the remaining coefficients are defined as

$$\begin{aligned}
\Gamma_2 &= 2\kappa_2\mathcal{C}_2^2,\\
\widetilde{\Gamma}_2 &= \tfrac{2}{3}\kappa_2\mathcal{C}_3^2,\\
\Gamma_3 &= 2\kappa_3\mathcal{C}_3^3.
\end{aligned} \tag{28}$$

Uncorrelated thermal gas

We can find an expression for the integrated n-particle point correlation function $\mathcal{C}_m^n \equiv \int d^3r\langle\hat{\psi}^{\dagger n}(\mathbf{r})\hat{\psi}^n(\mathbf{r})\rangle_m$ of Eq. (25) in terms of the n-th power of the single-particle density using the assumptions

1. the particles are independently distributed by a given thermal distribution with probability p_ν to occupy state $|\nu\rangle$,
2. the probability $p_\nu \ll 1$ for every ν and thus we may ignore the possibility for more than one particle to occupy the same state.

In this case we may write for the density operator

$$\hat{\rho}_m \approx \sum_{i_1,\ldots,i_m} p_{i_1}\cdots p_{i_m} a_{i_1}^\dagger\cdots a_{i_m}^\dagger|\mathrm{vac}\rangle\langle\mathrm{vac}|a_{i_m}\cdots a_{i_1} \tag{29}$$

$$= (\hat{\rho}_1)^m. \tag{30}$$

The correlation function then becomes

$$\langle\hat{\psi}^{\dagger n}(\mathbf{r})\hat{\psi}^{n}(\mathbf{r})\rangle_m = \mathrm{Tr}\hat{\rho}_m\hat{\psi}^{\dagger n}(\mathbf{r})\hat{\psi}^{n}(\mathbf{r}) \tag{31}$$

$$= \sum_{i_1,\ldots,i_m} p_{i_1}\cdots p_{i_m}\langle \mathrm{vac}|a_{i_m}\cdots a_{i_1}\hat{\psi}^{\dagger n}(\mathbf{r})\hat{\psi}^{n}(\mathbf{r})a^{\dagger}_{i_1}\cdots a^{\dagger}_{i_m}|\mathrm{vac}\rangle. \tag{32}$$

We can resolve the expectation value by commuting the field $\hat{\psi}(\mathbf{r})$ operators past the orbital creation operators towards the right (until they hit the vacuum) using

$$\left[\hat{\psi}(\mathbf{r}), a^{\dagger}_i\right] = \phi^*_i(\mathbf{r}), \tag{33}$$

which give us the value of the orbital function at position x. The n field operators generate $m(m-1)\cdot(m-n+1)$ terms, of which, however, $n!$ terms are identical. The same happens with the field creation operators $\hat{\psi}^{\dagger}(\mathbf{r})$ acting to the left. Only terms with identical content of orbitals will have non-vanishing overlap such that there are $\binom{m}{n}$ terms, but each has a prefactor $(n!)^2$ since it appears on both the left and right hand side. We are thus left with

$$\langle\hat{\psi}^{\dagger n}(\mathbf{r})\hat{\psi}^{n}(\mathbf{r})\rangle_m = (n!)^2\binom{m}{n}\left[\tilde{n}(\mathbf{r})\right]^n, \tag{34}$$

where

$$\tilde{n}(\mathbf{r}) = \sum p_i|\phi_i(\mathbf{r})|^2 = \frac{n(\mathbf{r})}{m}, \tag{35}$$

is the single-particle density normalised to 1.

For the integrated density we thus have

$${}^{\mathrm{th}}\mathcal{C}^n_m = (n!)^2\binom{m}{n}\int d^3x\left[\tilde{n}(\mathbf{r})\right]^n \tag{36}$$

$$= n!m(m-1)\cdots(m-n+1)\int d^3x\left[\tilde{n}(\mathbf{r})\right]^n \tag{37}$$

$$= \frac{n!m(m-1)\cdots(m-n+1)}{m^n}\int d^3x\left[n(\mathbf{r})\right]^n. \tag{38}$$

Specifically, for the 3-body term with $n=m=3$ we obtain

$${}^{\mathrm{th}}\mathcal{C}^3_3 = \frac{4}{3}\int d^3r\left[n(\mathbf{r})\right]^3. \tag{39}$$

The two-particle correlators become

$${}^{\mathrm{th}}\mathcal{C}^2_3 = 12\int d^3x\left[\tilde{n}(\mathbf{r})\right]^2 = 3\,{}^{\mathrm{th}}\mathcal{C}^2_2, \tag{40}$$

which implies $\Gamma_2 = \widetilde{\Gamma}_2$.

LINEAR MODEL ANALYTICAL SOLUTION

The linear loss-rate model [Eq. (2) in main paper in the form of Eq. (26) above] that describes the evolution of the loss events for three body dynamics is:

$$\begin{pmatrix}\dot{r_3}(t)\\ \dot{r_2}(t)\\ \dot{r_1}(t)\\ \dot{r_0}(t)\end{pmatrix} = \begin{bmatrix}-(\Gamma_3+3(\widetilde{\Gamma}_2+\Gamma_1)) & 0 & 0 & 0\\ 3\Gamma_1 & -(\Gamma_2+2\Gamma_1) & 0 & 0\\ 3\widetilde{\Gamma}_2 & 2\Gamma_1 & -\Gamma_1 & 0\\ \Gamma_3 & \Gamma_2 & \Gamma_1 & 0\end{bmatrix}\begin{pmatrix}r_3(t)\\ r_2(t)\\ r_1(t)\\ r_0(t)\end{pmatrix}. \tag{41}$$

The solutions to this system are used to fit to the experimental data in order to extract the rate coefficients Γ_j. Their general solutions are:

$$\begin{aligned}
r_3(t) &= A\exp[-(\Gamma_3+3\widetilde{\Gamma}_2+3\Gamma_1)t],\\
r_2(t) &= \frac{-3A\Gamma_1}{\Gamma_3+3\widetilde{\Gamma}_2-\Gamma_2+\Gamma_1}\exp[-(\Gamma_3+3\widetilde{\Gamma}_2+3\Gamma_1)t]+B\exp[-(\Gamma_2+2\Gamma_1)t],\\
r_1(t) &= -\alpha\exp[-(\Gamma_3+3\widetilde{\Gamma}_2+3\Gamma_1)t]-\beta\exp[-(\Gamma_2+2\Gamma_1)t]+C\exp(-\Gamma_1 t),\\
r_0(t) &= \left[-\Gamma_3 A+\left(\frac{3A\Gamma_1\Gamma_2}{\Gamma_3+3\widetilde{\Gamma}_2-\Gamma_2+\Gamma_1}\right)+\Gamma_1\alpha\right]\left(\frac{1}{\Gamma_3+3\widetilde{\Gamma}_2+3\Gamma_1}\right)\exp[-(\Gamma_3+3\widetilde{\Gamma}_2+3\Gamma_1)t]-C\exp(-\Gamma_1 t),\\
&\quad+(-\Gamma_2 B+\Gamma_1\beta)\left(\frac{1}{\Gamma_2+2\Gamma_1}\right)\exp[-(\Gamma_2+2\Gamma_1)t]+D,
\end{aligned} \tag{42}$$

where α & β are:

$$\alpha=\left(\frac{3A}{\Gamma_3+3\widetilde{\Gamma}_2+2\Gamma_1}\right)\left[\widetilde{\Gamma}_2-\left(\frac{2\Gamma_1^2}{\Gamma_3+3\widetilde{\Gamma}_2-\Gamma_2+\Gamma_1}\right)\right];\qquad \beta=\left(\frac{2B\Gamma_1}{\Gamma_2+\Gamma_1}\right), \tag{43}$$

and A, B, C and D are constants of integration evaluated from initial atom populations of zero, one, two, and three atoms in the trap, before collisions began. We estimate these initial populations by analyzing the flourescence collected by the Single Photon Counter Module with 'Wait Time' $= t = 0$ as described in the main text. The initial populations are:

$$\begin{pmatrix} r_3(0)\\ r_2(0)\\ r_1(0)\\ r_0(0)\end{pmatrix}=\begin{pmatrix}0.836\\0.022\\0.141\\0.001\end{pmatrix}. \tag{44}$$

THE TWO-BODY LOSS RATE COEFFICIENT

We would like to find Γ_2's dependence on $\omega_\perp$ assuming that the two-body loss rate coefficient K_2 is proportional to an integer power (m) of the tweezer beam intensity:

$$\Gamma_2\propto K_2\int n^2(\mathbf{r})\,d^3r\propto I^m\int n^2(\mathbf{r})\,d^3r. \tag{45}$$

Harmonic expansion of the tweezer potential result in $I\propto\omega_\perp^2$, and the density profile of a thermal gas given in the main text gives $\int n^2(\mathbf{r})\,d^3r\propto\omega_\perp^{3/2}$. Insertion into (45) yields:

$$\Gamma_2\propto\omega_\perp^{2m+3/2}. \tag{46}$$